Research Paper

Astragaloside IV Adjusts Circadian Rhythm Genes to Enhance Apoptosis in Mice Exhibiting Urticaria-Like Symptoms

ANJING CHEN, XURUI WANG[1], YAOBIN PANG, XUEER ZHANG, LI PENG AND JING GUO*

Department of Dermatology, Hospital of Chengdu University of Traditional Chinese Medicine, [1]Department of Chinese Medicine Surgery, Sichuan Provincial People's Hospital, University of Electronic Science and Technology of China, Chengdu, Sichuan 610072, China

Urticaria symptoms and disease severity exhibit a 24 h cycle, with circadian rhythms influencing skin tissue apoptosis. This study sought to evaluate the impact of astragaloside IV on core circadian gene expression and cell apoptosis in mice with urticaria-like lesions. Sixty mice were allocated to three groups at random, including a normal group (administered with saline), a model group (administered with ovalbumin and aluminum), and an astragaloside IV group (50 mg/kg/d). Each group was further subdivided into zeitgeber time 0 and zeitgeber time 12 subgroups. Allergic reactions, behavioral rhythms and histopathology were assessed in urticaria-like mice. Serum concentrations of immunoglobulin E, histamine and leukotriene B4 were determined by enzyme-linked immunosorbent assay; cell apoptosis was assessed by terminal deoxynucleotidyl transferase dUTP nick end labeling technique; the levels of protein of p53 and B-cell lymphoma 2 were analyzed by Western blot and immunohistochemistry, and reverse transcription quantitative-polymerase chain reaction was applied to determine messenger ribonucleic acid levels of brain and muscle ARNT-like, circadian locomotor output cycles kaput, period 2, and cryptochrome 1. The findings demonstrated that astragaloside IV significantly reduced allergic and inflammatory responses in urticaria-like mice and lowered serum inflammatory factors. Astragaloside IV also enhanced apoptosis in skin tissues by increasing p53 and decreasing B-cell lymphoma 2 levels. Furthermore, astragaloside IV elevated messenger ribonucleic acid levels of BMAL1, circadian locomotor output cycles kaput, and period 2, while reducing cryptochrome 1 expression in the suprachiasmatic nuclei. Mice showed a greater therapeutic response to astragaloside IV at zeitgeber time 12. In conclusion, astragaloside IV facilitates apoptosis and regulates circadian rhythm gene expression in urticaria-like mice, with its effects being dependent on the timing of administration.

Key words: Natural products, astragaloside IV, circadian rhythm, chronotherapy, apoptosis, allergic reactions

Urticaria, a prevalent cutaneous disorder, is characterized by localized edema resulting from the dilation of small blood vessels within the skin and mucosa, and an increase in permeability. It is clinically characterized by the presence of wheals of varying sizes along with pruritus and may be accompanied by angioedema. In the early stage of urticaria onset, mast cells are activated and undergo degranulation, releasing Histamine (HIS) and other vasoactive mediators such as prostaglandins, leukotrienes and cytokines, collectively triggering the occurrence of urticaria[1]. A previous review concluded that the symptoms' intensity and disease severity in numerous allergic conditions, including bronchial asthma, atopic eczema and chronic urticaria, exhibit a 24 h pattern[2]. In mammals, the circadian rhythm adheres to a 24 h light/dark cycle, originating from a central pacemaker situated within the Suprachiasmatic Nucleus (SCN). This nucleus, situated at the base of the hypothalamus, establishes the internal circadian rhythm by receiving light signals[2,3]. At the molecular level, Circadian Locomotor Output Cycles Kaput (CLOCK) and Brain and Muscle ARNT-Like-1 (BMAL1) heterodimers activate the transcription of the Period 2 (PER2) and Cryptochrome 1 (CRY1) genes. PER and CRY proteins then decrease their levels by restraining the activity of CLOCK and BMAL1. With additional post-translational modifications, this negative feedback loop produces a clock protein level with a roughly 24 h periodicity, which manifests as circadian

***Address for correspondence**
E-mail: guojing66@cdutcm.edu.cn

behavior and physiology[4]. Circadian rhythms regulate various activities, including apoptosis, cell cycle, energy metabolism, endocrine and immune functions[5]. Critically, it is well established that circadian rhythms can participate in the apoptotic process of skin tissues, which is considered crucial for skin physiology[6]. Apoptosis is the spontaneous and orderly death of genetically controlled cells aimed at maintaining homeostatic stability[7]. B-cell lymphoma 2 (Bcl-2) is a primary anti-apoptotic protein that blocks the initiation of the apoptotic process by blocking the release of apoptotic factors from mitochondria[8]. A prior investigation disclosed that the concentration of Bcl-2 was correlated to the mRNA expressions of PER2 and BMAL1[9]. p53, a crucial tumor suppressor protein, is known for its role in promoting apoptosis. Many studies suggested that p53 can regulate cellular apoptosis by interacting with circadian genes[10-12].

Antihistamines, corticosteroids and immunosuppressive agents are currently the primary treatment options for urticaria. Antihistamines block HIS receptors to reduce itching and inflammation. Corticosteroids function as potent anti-inflammatory agents, while immunosuppressive agents are reserved for severe cases of urticaria, targeting the immune system to reduce inflammation. However, these agents are associated with significant side effects, such as drowsiness, weight gain, osteoporosis and immunosuppression, which limits their long-term use. Hence, there is a pressing demand for a new therapeutic approach with a more favorable safety profile.

Astragaloside IV (AS-IV) is a purified compound weight saponin exist in the root of *Astragalus aleppicus* Boiss. (Fabaceae). It has been demonstrated that AS-IV has various beneficial properties, encompassing anti-inflammatory, anti-allergic and anti-thrombotic abilities[13,14]. Importantly, earlier investigations have indicated the strong anti-inflammatory and anti-allergic effects of AS-IV in asthma[15], allergic contact dermatitis[16] and allergic rhinitis[17]. However, the exact mechanism of AS-IV in the mouse models of Urticaria-like Lesions (ULs) sensitized by Ovalbumin (OVA)/Aluminum (Alum) remains unknown. Chronotherapy involves drug administration based on daily biological rhythms[18]. Previous studies have revealed that differences in administration time can influence the effects of medications[19,20], which provide us with a new perspective for treatment of urticaria. Circadian rhythm governs immune and allergic responses, with endogenous glucocorticoids serving as Zeitgebers. These glucocorticoids, receiving signals from the SCN, help synchronize the peripheral clock[21]. In animals active at night, serum glucocorticoid levels reach their maximum before and after the start of the active phase (between Zeitgeber Time (ZT)-12 and ZT16), and drop to their lowest point between ZT0 and ZT4[22]. Thus, this study evaluates the curative effects and probable underlying mechanisms of AS-IV at different time periods. ZT0 and ZT12 were chosen to be the administration time points.

This investigation elucidates the chronotherapeutic ability of AS-IV on circadian clock genes and apoptosis in urticaria animal models. Our results provide compelling evidence that AS-IV possesses remarkable therapeutic promise in treating urticaria by controlling the levels of circadian rhythm genes associated with apoptotic factors. Moreover, our investigation reveals that the administration of AS-IV at ZT12 yields more efficacy compared to ZT0. These discoveries open avenues for identifying new therapeutic targets in the management of urticaria.

MATERIALS AND METHODS

Drugs:

AS-IV (purity, ≥98 %) was purchased from Hefei Bomei Biotechnology; Co., Ltd., (Cat no: BZP0070).

Animals:

Approval for all animal experiments was granted by the Animal Ethics Committee of Hospital of Chengdu University of Traditional Chinese Medicine (No: 2020DL-004). In total, 120 male BALB/c mice (6 w old) were purchased in Chengdu Dashuo experimental animal Co., Ltd., (Cat no: SCXK-2015-030). Under optimal ventilation conditions, the mice were housed individually in cages equipped with running wheels, at 22°±2°, 40 %-60 % humidity in a colony room with a 12 h light/dark cycle (ZT0 means lights on at 7:00 am and ZT12 means lights off at 7:00 pm), and were provided with unlimited access to water and food *ad libitum*. Current study adhered to the Animal Research Reporting of *In Vivo* Experiments (ARRIVE) guidelines.

Animal model and treatments:

Sixty mice were acclimated in a 12 h Light-Dark (LD) rhythm and another 60 were acclimated in a fully Dark (DD) environment. After 14 d of adaptation, mice in

two different light regimes were, respectively and randomly, divided into three groups (n=20); a normal group (Normal Saline (NS)), a model group (OVA/Alum and NS), and an AS-IV group (OVA/Alum and AS-IV). Each group was further divided into ZT0 and ZT12 subgroups. Normal mice were randomly divided into four groups, designated as LD-ZT0 normal, DD-ZT0 normal, LD-ZT12 normal and DD-ZT12 normal. The model mice were designated as LD-ZT0 model, DD-ZT12 model, LD-ZT12 model, and LD-ZT12 model and AS-IV mice were designated as LD-ZT0 AS-IV, DD-ZT0 AS-IV, LD-ZT12 AS-IV and DD-ZT12 AS-IV. The sample size calculation was based on our previous study[23], which indicated that ten mice per group were necessary for this study.

To establish mouse models of ULs, the mice, except those in the control cohort, were intraperitoneally (i.p.) injected with a suspension of OVA (10 µg; Hefei Bomei Biotechnology Co., Ltd., Hefei, China; AL7512) and Alum (0.1 ml; Chron chemicals Co., Ltd., Chengdu, China; 21645-51-2) on d 0, 2, 4 and 14. At 24 h after the first injection with OVA and Alum, normal and modeled mice were orally administered with NS at ZT0 or ZT12 according to the feeding time of each group, while the mice of the AS-IV groups received AS-IV (50 mg/kg)[17,24] at ZT0 or ZT12 every day from d 1 to d 14. After that, in accordance with the guidelines set by the institutional animal care and use committee, cervical dislocation was performed to sacrifice the mice on d 15. Briefly, all mice were intraperitoneally anesthetized with 1 % sodium pentobarbital (45 mg/kg). Once the mice reached a deep state of unconsciousness with no reactions to stimuli, they were positioned in a supine posture on a stable surface. Firm pressure is applied at their base of the skulls, along with a sharp pinching and twisting of the thumb and index finger. At the same time, their tails were pulled backward, which causes rapid death. Then, their skin tissues were collected, and their eyeballs were removed for collecting blood samples (500 µl). The brain of the mice was extracted and encased in OCT before being rapidly frozen at -80°. Using the Leica CM1850 cryostat slicer, coronal brain sections of 100 µm were prepared, with a focus on collecting slices containing the SCN and other sub-hypothalamic regions. The middle area of the SCN was isolated using a 26G needle on a 1 ml syringe under magnification as previously described[25]. Then, the isolated SCN was frozen in liquid nitrogen for 24 h and subsequently transferred to a -80° refrigerator for storage.

Allergic reaction:

The hair color, appearance, water and food intake, sleep, urine output, body weight, scratching behavior, lip and tongue color, fur color glossiness, arched back, vertical hair, activity, stool and anal conditions of the mice were observed and recorded, and were used to assess the level of scratching and the intensity of skin lesions in mice. The allergic reaction score used was as follows; 0 means absence of indications; 1 means scratching and rubbing near the nose and head; 2 means reduced movement or remaining stationary with heightened breathing or puffiness around the eyes; 3 means audible breathing difficulties, struggling to breathe and bluish discoloration around the mouth and tail; 4 means lack of activity even when stimulated, shaking and seizures and 5 means fatality[26,27].

Behavioral rhythms:

Daily wheel-running activities and the circadian behavior of the mice before and after interventions were recorded. The Clocklab2 rhythm data acquisition system (ACT-500; Actimetrics) was used to continuously and dynamically monitor the wheel-running activities of mice and to collect the wheel-running activity data hourly. Matlab (Math Works, Inc.) was used to analyze the wheel running activity data for each group of mice over the 14 experimental days.

Pathological analysis:

The skin tissues were preserved in 4 % paraformaldehyde, embedded in paraffin and then sectioned. Next, the paraffin sections were routinely dewaxed, rehydrated, stained with hematoxylin for 10 min and counterstained with eosin for 2 min. Finally, the sections were dried, cleared and mounted. The slices were sealed, and the histological features were observed with a microscope at 100X magnification (BA400 Digital; MOTIC CHINA Group Co., Ltd.).

Mast cell detection:

Paraffin-embedded sections were conventionally deparaffinized, rehydrated, stained with 1 % toluidine blue aqueous solution and dehydrated through an alcohol gradient, xylene transparent, and neutral gum sealing. When observed microscopically at 100X magnification, the nuclei of mast cells were round or elliptic and colored dark blue, while the cytoplasm was filled with thick purplish red heterochromatic particles, which were mainly distributed in the

stroma. The mast cells had irregular shapes and released purple particles extracellularly.

Serum detection:

The blood specimens were subjected to centrifugation at 3000 g for 10 min at 4°, after centrifugation, the serum was transferred and stored at -80°. Enzyme-Linked Immunosorbent Assay (ELISA) kits (Cat no: ZC-38496, ZC-37956 and ZC-39061; ZCiBIO) were used to determine the amount of Immunoglobulin E (IgE), Leukotriene B4 (LTB4) and HIS in the serum, in compliance with the guidelines outlined by the manufacturer. First, antibodies against IgE, LTB4 and HIS were immobilized onto a 96-well microtiter plate. Second, the samples were introduced into each well, allowing IgE, LTB4 and HIS to bind to their respective antibodies immobilized on the solid-phase carrier. Third, antibodies against IgE, LTB4 and HIS were put in. After removing away the unbound biotin-labeled antibodies, Horseradish Peroxidase (HRP)-labeled avidin was added, followed by 3,3′,5,5′-Tetramethylbenzidine (TMB) substrate for chromogenic detection. Subsequently, the sample concentration was detected by measuring the absorbance (Optical Density (OD)) value at 450 nm using a microplate reader.

Terminal Deoxynucleotidyl Transferase dUTP Nick End Labeling (TUNEL) assay:

TUNEL kit (Servicebio Technology Co., Ltd., Cat no: G1507) was utilized to determine apoptosis, and the amount of apoptosis cells was recorded. Initially, paraffin-embedded sections underwent standard dewaxing and rehydration, followed by antigen retrieval facilitated by incubating with a proteinase K working solution (Wuhan Servicebio Technology Co., Ltd.; Cat no: G1205). Subsequently, the endogenous peroxidase activity was blocked with 3 % Hydrogen peroxide (H_2O_2). TUNEL and buffer from the aforementioned TUNEL kit were mixed at a 1:5:50 ratio. Thereafter, the sections underwent treatment with a combination of streptavidin-HRP and TBS-Tween at a dilution ratio of 1:200. Finally, samples were treated with 3,3'-Diaminobenzidine (DAB) chromogenic reagent and counterstained with hematoxylin staining solution. The quantity of apoptotic cells was counted by a light microscope at 400X magnification. Three arbitrary visual fields were chosen per section, and the relative proportion of apoptosis, defined as the percentage of apoptotic cells among the total cell count in each field, was counted. The average value of the apoptotic cell rate of each group was also determined[28].

Immunohistochemistry (IHC):

IHC was utilized to assess the levels of p53 and Bcl-2 proteins in mouse skin tissue. Briefly, paraffin-embedded sections were deparaffinized, rehydrated and incubated with antibodies against p53 (AB clonal Biotech Co., Ltd.; Cat no: A11232) or Bcl-2 (AB clonal Biotech Co., Ltd.; Cat no: A19693) at 4° overnight, followed by cultivation with biotinylated secondary antibodies and staining with a DAB (immunohistochemistry color development) kit (OriGene Technologies, Inc.; Cat no: ZLI9019). In total, three visual fields were randomly selected under 200X light microscope, three microscopic views were unpredictably chosen under a 200X magnification light microscope, and the Integrated OD (IOD) was employed for semi-quantitative scoring. The images were assessed by a second pathologist, who was unaware of the research data, applying image-pro plus 6.0 software (Media Cybernetics, Inc.).

Western blotting:

The skin tissue of the mice was cut into 30 mg with clean and disinfected scissors and lysed in ice-cold Radio-Immunoprecipitation Assay (RIPA) lysis buffer (Beyotime, P0013C, Beyotime Institute of Biotechnology, Shanghai, China) supplemented with protease and phosphatase inhibitor (Solarbio Life Sciences, China), broken by ultrasound and incubated on ice for 30 min. The protein lysate underwent centrifugation at 12 000 g for 10 min at 4° and the supernatant was harvested. Protein concentrations were quantified using the Bicinchoninic Acid (BCA) protein assay kit (Beyotime, P0012S, Beyotime Institute of Biotechnology, Shanghai, China). Total proteins were heated at 100° for 10 min in 5× loading buffer to induce denaturation. 20 mg of total protein in each lane underwent Sodium Dodecyl Sulphate-Polyacrylamide Gel Electrophoresis (SDS-PAGE) and subsequent transfer onto a Polyvinylidene Fluoride (PVDF) membrane (Merck Millipore Ltd., Germany). The membrane was sealed using 5 % milk powder solution for 2 h, followed by cultivation at 4° with antibodies against p53 (1:1000; Cat no: AP062; Shanghai Beyotime Biotechnology Co., Ltd.) or Bcl-2 (1:1000; Cat No: AB112; Shanghai Beyotime Biotechnology Co., Ltd.) overnight. Following this, the membrane underwent Tris-Buffered Saline with 0.1 % Tween® 20 (TBST) detergent washing and subsequent incubation with the secondary antibody

(1:5000, Goat anti-mice IgG, Cat no: GB23301, Servicebio) or (1:5000, Goat anti-rabbit IgG, Cat no: G1213, Servicebio) at 37° for 1 h. Thereafter, the membrane underwent three washes with TBST for 5 min each, followed by visualization using Enhanced Chemiluminescence (ECL) liquid (Biosharp Life Sciences, China). The gray values of each blotted-protein band were calculated by ImageJ software. The relative protein contents were expressed as the proportion between the gray values of the target protein strip and Glyceraldehyde 3-Phosphate Dehydrogenase (GAPDH).

Reverse Transcription-quantitative Polymerase Chain Reaction (RT-qPCR):

The collected mouse brain tissue was stored at -80° until processed, and total RNA from tissues was purified using the total RNA isolation kit (Foregene Biotechnology Co., Ltd., Cat no: RE-03014). We evaluated the concentration and purity ratios of RNA using the NanoDrop 2000/2000c Spectrophotometer (Thermo Fisher Scientific, Inc.). Next, complementary Deoxyribonucleic Acid (cDNA) was synthesized from RNA applying a reverse-transcriptase, and the target fragment was amplified using cDNA as a template. The thermocycling proceeded with an initial denaturation at 95° for 30 s; followed by 45 cycles of denaturation at 95° for 6 s and annealing at 55° for 30 s. Finally, there was an extension step at 72° for 30 s. β-actin was utilized as the positive reference gene. Applying the Quant Studio RT-PCR Software (Thermo Fisher Scientific, Inc.) to analyze the threshold Cycle (C_t) values of every sample detected during the PCR procedure and the $2^{-\Delta\Delta Ct}$ approach was applied to calculate the relative mRNA levels[29]. The variability inter-technical replicates and inter-plates were analyzed by calculating the Coefficient of Variation (CV) of the C_t values for each gene. The CV values were <5 %, indicating good reproducibility of the assay. Table 1, shows the designed primer sequences (National Center for Biotechnology Information Search database).

Statistical analysis:

Statistical analyses utilized Statistical Package for the Social Sciences (SPSS) v26.0 software (IBM Corp.). All experiments were separately performed thrice and the data is displayed as the mean±standard deviation. Group disparities were assessed *via* Analysis of Variance (ANOVA), and post hoc tests using Tukey's and Dunnett's T3 methods were conducted. Statistical significance was defined at a threshold of *$p<0.05$.

RESULTS AND DISCUSSION

No abnormalities were observed in the normal mice groups. After sensitization, mice exhibited varying degrees of pruritus, thrusting, dorsal arching, piloerection and decreased dietary intake and activity. Treatment with AS-IV ameliorated the aforementioned clinical symptoms to varying extents. No mice died during the experiment. The allergic reaction score of the mice is depicted in fig. 1A. Remarkably, no notable distinction was observed between the ZT0 and ZT12 group.

Pathological irregularities were distinctly evident in biopsies of urticarial lesions in model mice when contrasted with the skin of normal mice. The cutaneous tissues in the model groups exhibited incompleteness, with disordered dermal edema and the arrangement of collagen fibers in the dermal papilla layer. There was serious exudation; the collagen fiber staining was lightened, and the gap between collagen fibers was widened. Blood vessels showed dilation, with limited inflammatory cells infiltration around them. AS-IV significantly improved the pathological morphology of UL mice, as evidenced by the reduction in dermal edema, collagen bundled distance, and capillary dilation (fig. 1B). In summary, AS-IV was able to improve UL pathological changes in mice. One of the most common triggering factors of urticaria is mast cell degranulation induced *via* the high-affinity IgE receptor[30]. Therefore, toluidine blue staining was performed to examine whether AS-IV could effectively ameliorate mast cell activation. Normal mice skin exhibited few purplish-red mast cells. A significantly higher number of released mast cells and granules were observed in the model cohort than in the normal cohort, indicating an obvious type I allergic reaction in UL mice. After used AS-IV, the quantity of mast cells and degranulation in the skin tissue of mice significantly decreased (fig. 2A and fig. 2B). Hence, AS-IV exhibited notable capability in reducing mast cell infiltration and inhibiting the heightened degranulation reaction. One of the most common triggering factors of urticaria is mast cell degranulation induced *via* the high-affinity IgE receptor[30]. Therefore, toluidine blue staining was performed to examine whether AS-IV could effectively ameliorate mast cell activation. Normal mice skin exhibited few purplish-red mast cells. A significantly higher number of released mast cells and granules were observed in the model cohort than

in the normal cohort, indicating an obvious type I allergic reaction in UL mice. After used AS-IV, the quantity of mast cells and degranulation in the skin tissue of mice significantly decreased (fig. 2A and fig. 2B). Hence, AS-IV exhibited notable capability in reducing mast cell infiltration and inhibiting the heightened degranulation reaction.

We calculated the average activity of mice (n=10) in each group. In the LD 12/12 cycle grouping, mice in the normal group had regular activity tracks (fig. 3A), but in the model group, the activity patterns of the UL mice were more widely distributed, exhibiting sudden and unpredictable changes under free-running conditions. On the 2nd, 3rd, 4th, 5th, 6th and 10th d, the activities of mice showed abnormal circadian rhythm, with more activities recorded in the light environment (of note, mice are nocturnal animals). The total activity decreased for 14 d, leading to a significant decrease in the dark/light activity ratio (fig. 3B), indicating fragmented rest-activity rhythms and unstable circadian rhythms. The round-running activity of AS-IV group mice eliminated this trend, and the drug administration at ZT12 time showed a better activity effect. In LD, the diurnal frequency of mice was maintained in the light cycle (fig. 3C). In the DD group, the circadian rhythm shifted forward, and a noteworthy reduction in the amplitude of the rhythm was noted ($p<0.05$), indicating that resting activity rhythm was fragmented and less robust, and the overall activity of the mice was markedly reduced (fig. 3D), signifying an impact on the circadian rhythm pattern of mouse behavior. After AS-IV treatment, the activity tracking of mice tended to a stable rhythm, and mice in the ZT12 group exhibited significantly heightened mobility and a more consistent trajectory ($p<0.01$).

TABLE 1: PRIMER SEQUENCES

Accession number	Gene	Size (bp)	Upstream (5'-3')	Downstream (5'-3')
NM_007393.5	β-actin	187	GAAGATCAAGATCATTGCTCC	TACTCCTGCTTGCTGATCCA
NM_011065.5	PER2	174	AAGTGACCTGCTCAACCTCCTTCTGG	AACTGCTCGCTTTCCTCCGTGTCTG
NM_007771.4	CRY1	218	TGAGGCTGGCGTGGAAGTCATCGT	TGGCATCTCCAGTGGCTCCATCTTG
NM_007489.4	BMAL1	164	AGTGGTGTGGACTGCAATCGCAAGAG	TGAACAGCCATCCTTAGCACGGTGAG
NM_007715.3	CLOCK	184	TCCAAGTCAGACACCGAGCACTCTCA	TGTGGCGAAGGTAGGATAGGCAGTCA

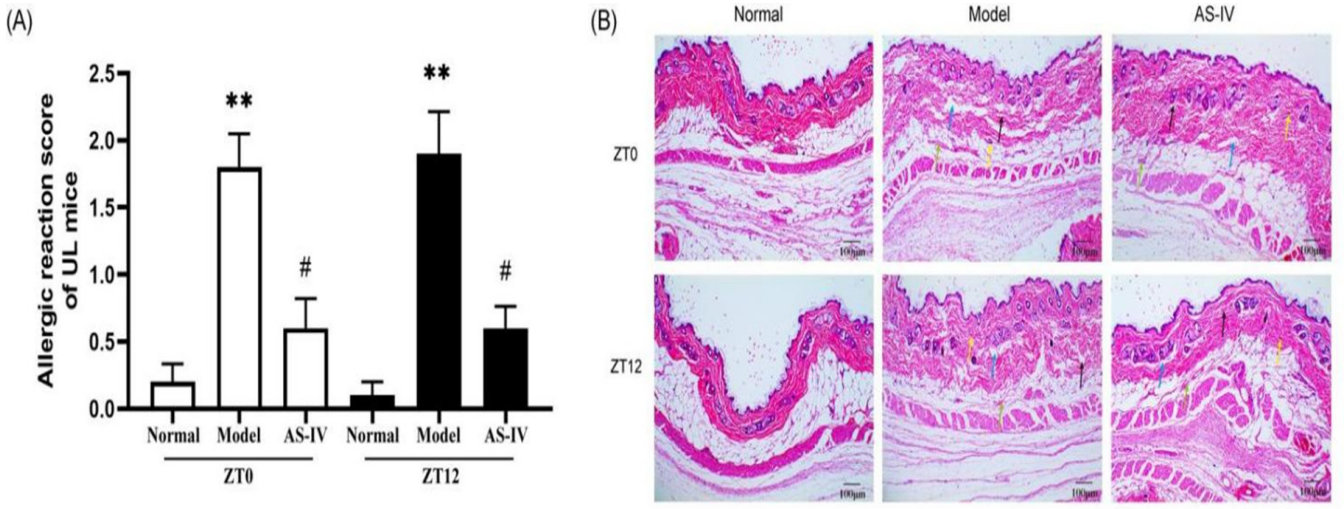

Fig. 1: (A): AS-IV ameliorates the allergic reaction and urticaria histopathology in mice and (B): Dorsal skin from mice in three groups was stained using hematoxylin and eosin (magnification, 100X). The blue arrow points to dermal edema, the black arrow points to widening of collagen fiber bundles, the green arrow points to telangiectasia and the yellow arrow points to inflammatory cells

Note: **p<0.01 *vs.* normal group and #p<0.05 *vs.* model group. The data was represented as mean±Standard Error of the Mean (SEM) (n=10)

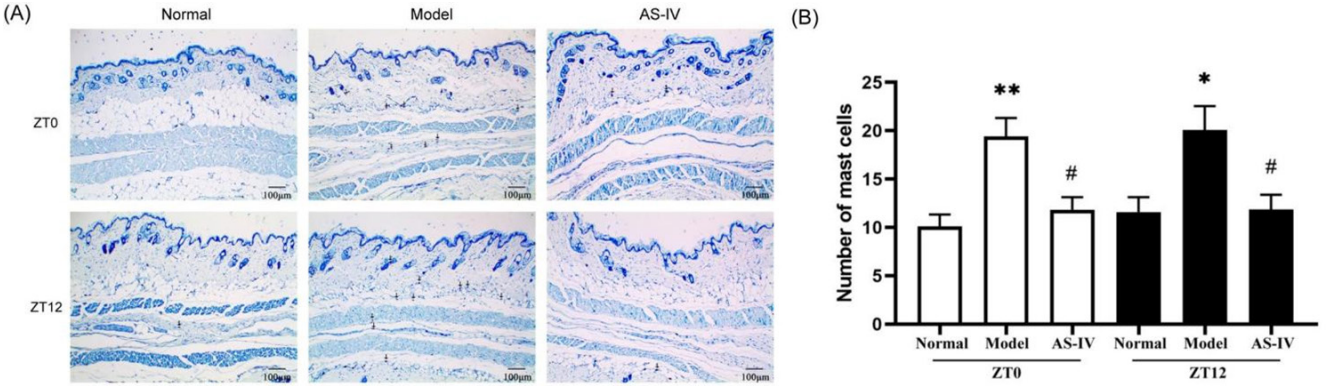

Fig. 2: AS-IV inhibits mast cell infiltration and degranulation, (A): Images illustrating mast cells stained with toluidine blue in dorsal skin of mice (100X) and (B): Mast cell density in the skin (n=10)
Note: *p<0.05, **p<0.01 *vs*. normal cohort and #p<0.05 *vs*. model cohort. The data was represented as mean±SEM

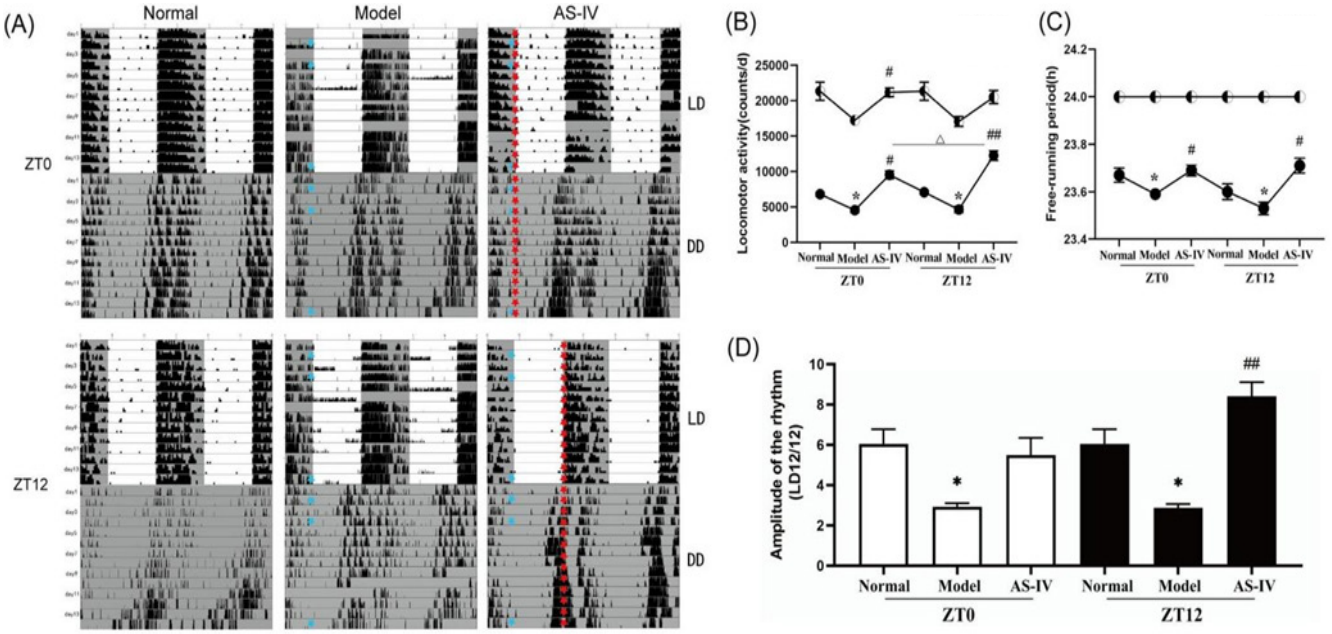

Fig. 3: AS-IV modulates the circadian behavior of mice with ULs, (A): Representative locomotor activity records of each group; (B): Effect of AS-IV on activity of model mice; (C): The free-running period of the locomotor activity rhythm in each group and (D): Ratio of night/day activities in LD group
Note: The data was portrayed as the mean±SEM (n=10). *p<0.05 *vs*. normal group; #p<0.05, ##p<0.01 *vs*. model group and Δp<0.05 *vs*. ZT0 AS-IV group. (LD): Light-Dark band and (DD): Black band-black band, (B and C): (-●-): LD and (-●-): DD

It has been reported that mast cells play an important role in inflammation by releasing various inflammatory mediators, including HIS, LTB4, mast cell-specific proteases and other compounds[31]. IgE is a clinical indicator for diagnosing urticaria allergy. As shown in fig 4A-fig. 4C, mice from the model groups exhibited markedly increased levels of IgE and HIS in serum compared to those in the corresponding normal cohort. Treatment of AS-IV at ZT12 resulted in observably decreased amount of IgE and HIS. Meanwhile, AS-IV treatment resulted in a decreasing trend for the levels of LTB4. Collectively, the increase in inflammatory cytokines was eliminated after AS-IV treatment, and administering AS-IV at ZT12 was more effective than at ZT0.

An increasing number of recent studies use methods to promote cell apoptosis to treat diseases such as psoriasis, skin cancer and allergic reactions[32,33]. In this study, nuclear staining was utilized to identify apoptosis-positive cells, denoted by arrows. The cells undergoing apoptosis included mast cells and corneocytes (fig. 5A). The TUNEL assay revealed a significant decrease in apoptosis in UL mice skin tissues, while mice in the AS-IV groups exhibited a significantly increased rate of apoptosis in their UL skin tissues compared to the model groups. Furthermore, AS-IV caused an observably higher amount of TUNEL-positive cells in specimens collected at ZT12 than those obtained at ZT0 (fig. 5B).

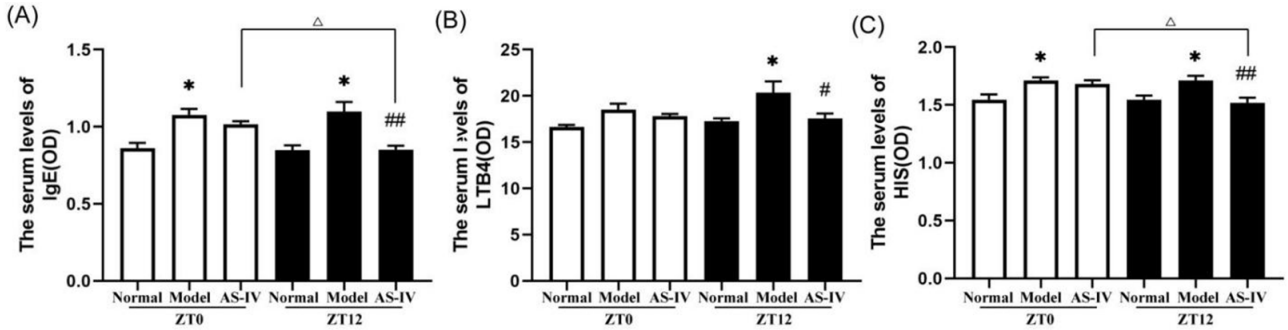

Fig. 4: AS-IV reduces the serum amount of (A): Immunoglobulin E; (B): Leukotriene B4 and (C): Histamine in mice with urticaria-like lesions

Note: *p<0.05 *vs.* normal group; #p<0.05 and ##p<0.01 *vs.* model group and Δp<0.05 *vs.* ZT0 AS-IV group. The data was portrayed as the mean±SEM (n=10)

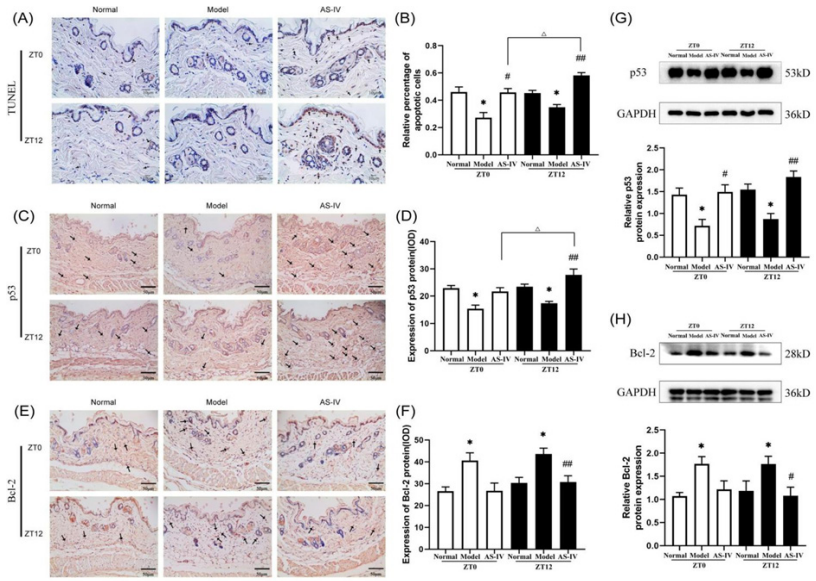

Fig. 5: AS-IV promotes cell apoptosis, increases the expression level of p53 and decreases that of Bcl-2 in the skin of mice with urticaria-like lesions

Note: *p<0.05 *vs.* normal group; #p<0.05 and ##p<0.01 *vs.* model group

Representative TUNEL images of apoptosis in the dorsal skin of mice (400X). Western blot analysis images revealing the expression of (G) p53 and (H) Bcl-2 in the dorsal skin of mice.

p53 is central in apoptotic cell death and intrinsic apoptotic pathways after DNA damage[34]. Several biological pathways are involved in regulating p53, including the cell cycle, DNA damage, apoptosis and glucose metabolism[35]. p53 has the function of inducing cell apoptosis and halting cell cycle. Positive p53 staining was observed in the cytoplasm and reflected as brownish-yellow granules (fig. 5C). Western blot and IHC analyses revealed a reduced expression of p53 protein in normal mice, whereas an even lower level of p53 protein was evident in the skin tissues of model mice (fig. 5D-fig. 5G). In contrast, p53 expression was enhanced in UL mice treated with AS-IV. Among them, the ZT12 AS-IV group showed the most significant changes. It is known that the Bcl-2 family of proteins is a key regulator of the mitochondrial response to apoptotic cues[36]. Controlling the permeation of the mitochondrial membrane, Bcl-2 regulates cell apoptosis and exerts an anti-apoptotic effect. A previous study reported that inhibiting Bcl-2 induced mast cell apoptosis[37]. The expression of the Bcl-2 protein in the cytoplasm is represented by the brownish-yellow particles (fig. 5E). However, the Bcl-2 level of ZT0 and ZT12 model groups was overexpressed than that of ZT0 and ZT12 normal groups ($p<0.05$). Furthermore, the concentration of Bcl-2 protein in the ZT0 and ZT12 AS-IV groups was remarkably lower than that of model groups ($p<0.05$). These findings suggest dosing AS-IV may promote apoptosis by downregulating the level of Bcl-2 (fig. 5F-fig. 5H).

The circadian clock is essential in controlling both local and systemic allergic responses. Previous studies have revealed circadian rhythms in IgE/mast cell-mediated allergic responses, such as Passive Cutaneous Anaphylactic (PCA) and Passive Systemic Anaphylactic (PSA) reactions. The core clock genes, including PER2, CLOCK and BMAL1, influence these rhythms[38,39]. In addition, it is suggested that circadian rhythms modulate the apoptosis procedure in diverse tissues[40]. To clarify whether the circadian rhythm is related to apoptosis in UL mice model, the mRNA expression of BMAL1, CLOCK, PER2 and CRY1 in the SCN and peripheral skin tissue of mice were detected in this study. All sample extractions were completed at the ZT0 time point. Notably, our findings indicate that, in the control cohort, no notable variances were observed in gene expression patterns between the sampled time points. In contrast, in model group, an evident reduction in the gene expression patterns of BMAL1, CLOCK and PER2 was observed relative to the normal group. Specifically, CLOCK expression was memorably downregulated ($p<0.05$), while PER2 expression was extremely significantly downregulated ($p<0.01$). Furthermore, we observed a significant upregulation of CRY1 expression ($p<0.01$). Trends in circadian core genes are synchronized in SCN and skin tissue. In the skin tissue, the gene expression of CLOCK in the model group markedly decreased compared with normal cohort ($p<0.01$), whereas CRY1 was very significantly upregulated ($p<0.01$). Although the suppression of BMAL1 and PER2 mRNA were also observed in the skin tissue of UL mice, the results were not statistically significant. Previous studies indicated that localized inflammation triggered alternations in the levels of PER2 and BMAL1, and in current experiment, as a consequence of upregulated inflammatory cytokines, the model group exhibited a potential augmentation in PER2 mRNA, while a decline in BMAL1 mRNA was observed[41,42]. CRY1 is an ancient and evolutionarily conserved protein which inhibits CLOCK/BMAL1 transactivation by creating a dimeric complex alongside PER[43]. High CRY1 expression in the mice model cohort attenuated the amount of BMAL1 and CLOCK. After AS-IV intervention, the pathological changes were significantly reversed and the reversal effect of the ZT12 group was better than that of ZT0 (fig. 6A-fig. 6H).

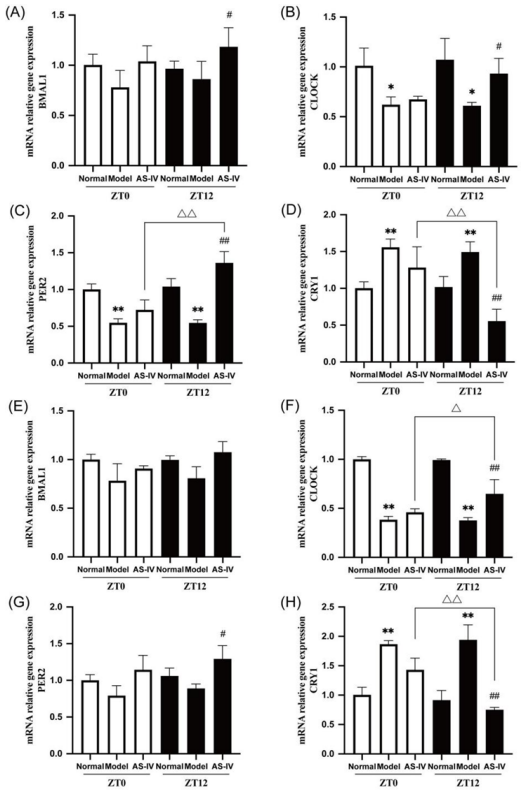

Fig. 6: AS-IV upregulates BMAL1, CLOCK and PER2 mRNA levels and downregulates CRY1 mRNA levels in the (A-D): Supra-chiasmatic nucleus and (E-H): Skin of mice, reverse transcription-quantitative PCR analysis of the mRNA expression levels in SCN (n=6) and skin tissue (n=3)

Note: *p<0.05 and **p<0.01 compared to normal group; #p<0.05 and ##p<0.01 compared to model group and Δp<0.05 and ΔΔp<0.01 compared to ZT0 AS-IV group. The data was portrayed as the mean±SEM

This investigation revealed that AS-IV ameliorated the skin pathological morphology of UL mice, reducing capillary dilation, the distance of the collagen bundle and edema. AS-IV also inhibited mast cell infiltration and degranulation, along with lowering IgE, LTB4 and HIS levels in the blood of UL mice (fig. 7). The amplitude of the rhythm in the model group mice under the LD environment was dramatically lower than that in the normal group, and the mice's activity was drastically reduced, indicating disturbed circadian rhythm. Mice housed in a DD environment showed a significantly shortened circadian rhythm with a forward phase shift, consistent with previous studies[44,45]. The study evaluated the drug efficacy at two opposite times, ZT0 and ZT12, in UL mice models. After AS-IV treatment, the amplitude and robustness of the circadian rhythm in mice returned to a normal level.

Compared to conventional urticaria treatments like antihistamines and corticosteroids, AS-IV presents a unique mechanism of action by modulating circadian rhythm genes, suggesting a potential for sustained and long-term therapeutic effects. While antihistamines address symptoms, their efficacy may wane over time, necessitating higher doses or additional treatments. Corticosteroids and immunosuppressive agents, though potent in anti-inflammatory effects, come with significant side effects, limiting long-term use. In comparison, AS-IV may offer a more favorable safety profile, providing a complementary approach to reduce inflammation and promote apoptosis. However, further studies are necessary to identify potential synergies with other therapies and compare AS-IV's safety and efficacy with existing treatment of urticaria.

Promoting apoptosis is one of the therapeutic strategies to eliminate activated eosinophils and lymphocytes in allergic diseases through drugs capable of inducing apoptosis in these inflammatory cells[46]. In this study, TUNEL results indicated a lower apoptosis index in the model group, while AS-IV treatment increased apoptosis in skin tissue, accompanied by an elevation in p53 and a reduction in Bcl-2. These findings show the potential of AS-IV to enhance apoptosis in UL mice.

The circadian system regulates almost all cellular physiological states, including cell cycle, DNA repair and apoptosis[40]. Dysregulated the core circadian gene PER2 level was linked to imbalances in cell proliferation and apoptosis. The pro-apoptotic protein p53 can interact with a regulatory sequence located within the PER2 promoter domain, which coincides with an E-box, consequently impeding transcription mediated by the CLOCK/BMAL1 complex[47]. In this study, the down-regulation of PER2 in the SCN of UL mice significantly decreased p53 protein expression in the skin, increased Bcl-2 protein expression and inhibited apoptosis.

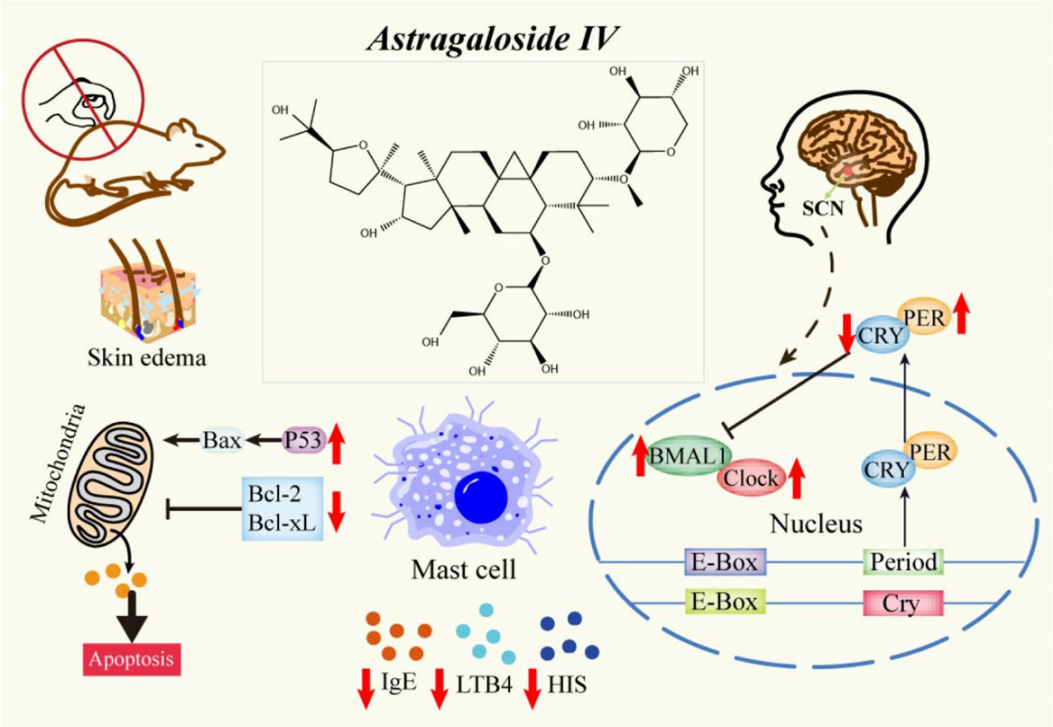

Fig. 7: Mechanism of AS-IV in alleviating the circadian rhythm of skin lesions and apoptosis in UL mice

AS-IV intervention significantly upregulated PER2 expression, along with p53. The study also found an increase in Bcl-2 protein in the skin of UL mice, a decrease in p53 protein, and the inhibition of apoptosis when PER2 expression was low in model group mice. Conversely, PER2 overexpression in the AS-IV groups led to increased apoptosis, possibly *via* the inhibition of Akt phosphorylation[36]. Moreover, p53 has been shown to interact directly with the circadian rhythm core genes BMAL1, CRY and PER. BMAL1 and CRY regulate the activity of the p53 promoter, and CRY mutations can downregulate p53 activity[34,48]. The current study reveals a trend of decreasing levels in BMAL1 and CLOCK, along with increased CRY1 levels in the model groups. Conversely, AS-IV treatment led to an increased expression of BMAL1 and CLOCK but a decreased level of CRY1. This consequently resulted in decreased Bcl-2 expression, increased p53 expression and enhanced apoptosis. Notably, the ZT12 AS-IV group exhibited the most pronounced alterations compared to the other evaluated groups. These results align with a prior report, which indicated that Bcl-2 proteins can either promote or inhibit apoptosis based on BMAL1 expression levels[49]. Collectively, these findings suggest that changes in circadian rhythm genes may impact apoptosis-related indicators. AS-IV can alleviate allergic reactions in UL mice by promoting apoptosis, with a more pronounced effect when administered at ZT12. The expression of circadian rhythm genes may contribute to variations in therapeutic effect at different times.

Chronotherapy involves the administration of drugs at specific times and does that align with the body's biological rhythm to optimize efficacy and minimize toxic reactions[50]. For instance, administering aspirin at night has been shown to reduce the occurrence rate of morning cardiovascular events, including myocardial infarction, in patients with hypertension[51]. In this study, AS-IV demonstrated a more favorable effect on UL mice when administered at ZT12 compared to ZT0, resulting in improved skin pathology, reduced mast cell degranulation, normalized wheel-running movement, decreased serum IgE and histamine levels and increased apoptosis. The ZT12 AS-IV group also showed more significant changes in apoptosis, p53 protein and mRNA levels of circadian rhythm genes PER2, CLOCK and CRY1 compared to the ZT0 group. Nonetheless, the underlying mechanism of chronopharmacology is not fully understood and may involve multiple factors, including the pharmacokinetic mechanism, the temporal rhythms of drug action associated with tissue sensitivity, rhythmic changes in receptor sensitivity, drug affinity and receptor density. Although our study suggests a significant association between chronopharmacology and animal species, additional exploration is necessary to elucidate more exact mechanisms.

This study revealed that urticaria disrupts the host's biological clock to a considerable extent, and administering AS-IV orally at two circadian intervals (ZT0 and ZT12) mitigated allergic response, histopathology, mast cell infiltration and inflammatory cytokines expression of UL mice and regulate their circadian behaviors. Notably, the ZT12 AS-IV treatment is more efficacious than that of ZT0. Nevertheless, certain constraints were observed. For example, the comprehensive mechanism of therapeutic abilities of AS-IV on regulating circadian rhythm and apoptosis remains to be clarified. Moreover, as the pathogenesis of urticaria is modulated by multiple processes and target cells, we would explore the detailed mechanisms of proapoptotic effects and the optimal administration time of AS-IV *in vitro* in subsequent studies. In summary, this study confirms the therapeutic potential of AS-IV in treating urticaria and sheds light on the relationship between urticaria-like allergic reactions, circadian rhythms and apoptosis, thereby expanding our understanding of urticaria chronotherapy. These observations may lay the groundwork for using chronotherapy as an innovative strategy for treating urticaria.

Ethical approval:

Ethical approval to report this case was obtained from the Animal Ethics Committee of Hospital of Chengdu University of Traditional Chinese Medicine (No: 2020DL-004).

Author's contributions:

Conceptualization by Jing Guo and Anjing Chen; validation by Xueer Zhang and Li Peng; methodology was done by Anjing Chen and Jing Guo; formal analysis by Anjing Chen, Yaobin Pang and Xurui Wang; investigation by Anjing Chen and Yaobin Pang; resources by Jing Guo, Anjing Chen and Li Peng; software was done by Xueer Zhang and Li Peng; data curation by Xurui Wang and Xueer Zhang; writing original draft by Anjing Chen, Yaobin Pang and Xurui Wang; writing review editing by Anjing Chen, Yaobin Pang and Xurui Wang; visualization by Xurui Wang and Yaobin Pang; supervision by Jing

Guo; project administration by Jing Guo and funding acquisition was done by Jing Guo. Anjing Chen and Xurui Wang have contributed equally to this work.

Funding:

This work was supported by the National Natural Science Foundation of China (No: 81873310 and 82074443), the "Young Qi Huang Scholars" from the State Administration of Traditional Chinese Medicine (no: 2022-256), Natural Science Foundation of Sichuan Province (no: 24NSFSC6525), the project of "Xing-lin Scholars" of Chengdu University of Traditional Chinese Medicine (Grant no: CGZH2018001, QNXZ2019017 and QNXZ2020003), the "Hundred Talents Program" of the Hospital of Chengdu University of TCM (Grant No: 21-L03 and 22-B09), the Science and Technology Developmental Foundation of the Hospital of Chengdu University of TCM (Grant no: 19TS03), Chengdu University of Traditional Chinese Medicine "Foundation Improvement Project" (2023-4), Sichuan Provincial People's Hospital Foundation Project (No: 2023QN12).

Conflict of interests:

The authors declared no conflict of interests.

REFERENCES

1. Guo C, Saltoun C. Urticaria and angioedema. Allergy Asthma Proc 2019;40:6.
2. Paganelli R, Petrarca C, di Gioacchino M. Biological clocks: Their relevance to immune-allergic diseases. Clin Mol Allergy 2018;16:1-8.
3. Kofuji P, Mure LS, Massman LJ, Purrier N, Panda S, Engeland WC. Intrinsically photosensitive Retinal Ganglion Cells (ipRGCs) are necessary for light entrainment of peripheral clocks. PloS One 2016;11(12):e0168651.
4. Tomita T, Miyazaki K, Onishi Y, Honda S, Ishida N, Oishi K. Conserved amino acid residues in C-terminus of PERIOD 2 are involved in interaction with CRYPTOCHROME 1. Biochim Biophys Acta 2010;1803(4):492-8.
5. Su X, Chen D, Yang K, Zhao Q, Zhao D, Lv X, *et al.* The circadian clock gene PER2 plays an important role in tumor suppression through regulating tumor-associated genes in human oral squamous cell carcinoma. Oncol Rep 2017;38(1):472-80.
6. Luengas-Martinez A, Paus R, Iqbal M, Bailey L, Ray DW, Young HS. Circadian rhythms in psoriasis and the potential of chronotherapy in psoriasis management. Exp Dermatol 2022;31(11):1800-9.
7. Hengartner MO. The biochemistry of apoptosis. Nature 2000;407(6805):770-6.
8. Chao DT, Korsmeyer SJ. Bcl-2 family: Regulators of cell death. Ann Rev Immunol 1998;16(1):395-419.
9. Granda TG, Liu XH, Smaaland R, Cermakian N, Filipski E, Sassone-Corsi P, *et al.* Circadian regulation of cell cycle and apoptosis proteins in mouse bone marrow and tumor. FASEB J 2005;19(2):1-22.
10. Zeng ZL, Wu MW, Sun J, Sun YL, Cai YC, Huang YJ, *et al.* Effects of the biological clock gene Bmal1 on tumour growth and anti-cancer drug activity. J Biochem 2010;148(3):319-26.
11. Lee JH, Sancar A. Regulation of apoptosis by the circadian clock through NF-κB signaling. Proc Natl Acad Sci 2011;108(29):12036-41.
12. Wang Q, Liu H, Wang Z, Chen Y, Zhou S, Hu X, *et al.* Circadian gene Per3 promotes astroblastoma progression through the P53/BCL2/BAX signalling pathway. Gene 2024;895:147978.
13. Zhao J, Yang P, Li F, Tao L, Ding H, Rui Y, *et al.* Therapeutic effects of astragaloside IV on myocardial injuries: Multi-target identification and network analysis. PLoS One 2012;7:e44938.
14. Li M, Qu YZ, Zhao ZW, Wu SX, Liu YY, Wei XY, *et al.* Astragaloside IV protects against focal cerebral ischemia/reperfusion injury correlating to suppression of neutrophils adhesion-related molecules. Neurochem Int 2012;60(5):458-65.
15. Huang X, Tang L, Wang F, Song G. Astragaloside IV attenuates allergic inflammation by regulation Th1/Th2 cytokine and enhancement $CD4^+$ $CD25^+$ Foxp3 T cells in ovalbumin-induced asthma. Immunobiology 2014;219(7):565-71.
16. Bao KF, Yu X, Wei X, Gui LL, Liu HL, Wang XY, *et al.* Astragaloside IV ameliorates allergic inflammation by inhibiting key initiating factors in the initial stage of sensitization. Sci Rep 2016;6(1):38241.
17. Li K, Chen Y, Jiang R, Chen D, Wang H, Xiong W, *et al.* Protective effects of astragaloside IV against ovalbumin-induced allergic rhinitis are mediated by T-box protein expressed in T cells/GATA-3 and forkhead box protein 3/retinoic acid-related orphan nuclear receptor γt. Mol Med Rep 2017;16(2):1207-15.
18. Slat EA, Sponagel J, Marpegan L, Simon T, Kfoury N, Kim A, *et al.* Cell-intrinsic, Bmal1-dependent circadian regulation of temozolomide sensitivity in glioblastoma. J Biol Rhythms 2017;32(2):121-9.
19. Yoshioka H, Ohishi R, Hirose Y, Torii-Goto A, Park SJ, Miura N, *et al.* Chronopharmacology of dapagliflozin-induced antihyperglycemic effects in C57BL/6J mice. Obes Res Clin Pract 2019;13(5):505-10.
20. Flo A, Cambras T, Díez-Noguera A, Calpena A. Melatonin pharmacokinetics after transdermal administration changes according to the time of the day. Eur J Pharm Sci 2017;96:164-70.
21. Shimba A, Ikuta K. Glucocorticoids regulate circadian rhythm of innate and adaptive immunity. Front Immunol 2020;11:545780.
22. Le Minh N, Damiola F, Tronche F, Schütz G, Schibler U. Glucocorticoid hormones inhibit food-induced phase-shifting of peripheral circadian oscillators. EMBO J 2001.
23. Guo J, Peng L, Zeng J, Zhang M, Xu F, Zhang X, *et al.* Paeoniflorin suppresses allergic and inflammatory responses by promoting autophagy in rats with urticaria. Exp Ther Med 2021;21(6):1.
24. Yang X, Wang F. The effect of astragaloside IV on JAK2-STAT6 signalling pathway in mouse model of ovalbumin-induced asthma. J Anim Physiol Anim Nutr 2019;103(5):1578-84.
25. Savelyev SA, Larsson KC, Johansson AS, Lundkvist GB. Slice preparation, organotypic tissue culturing and luciferase recording of clock gene activity in the suprachiasmatic nucleus. J Vis Exp 2011(48):e2439.
26. Li XM, Wang QF, Schofield B, Lin J, Huang SK, Wang Q. Modulation of antigen-induced anaphylaxis in mice by a

traditional Chinese medicine formula, Guo Min Kang. Am J Chin Med 2009;37(1):113-25.
27. Kumar Gupta R, Kumar S, Gupta K, Sharma A, Roy R, Kumar Verma A, *et al.* Cutaneous exposure to clinically-relevant pigeon pea (*Cajanus cajan*) proteins promote Th2 sensitization and IgE-mediated anaphylaxis in Balb/c mice. J Immunotoxicol 2016;13(6):827-41.
28. Duan WR, Garner DS, Williams SD, Funckes-Shippy CL, Spath IS, Blomme EA. Comparison of immunohistochemistry for activated caspase-3 and cleaved cytokeratin 18 with the TUNEL method for quantification of apoptosis in histological sections of PC-3 subcutaneous xenografts. J Pathol 2003;199(2):221-8.
29. Livak KJ, Schmittgen TD. Analysis of relative gene expression data using real-time quantitative PCR and the $2^{-\Delta\Delta CT}$ method. Methods 2001;25(4):402-8.
30. Hayashi T, Fujii T. Acute uriticaria-like lesions in allergen-unexposed cutaneous tissues in a mouse model of late allergic rhinitis. Int J Exp Pathol 2008;89(3):188-200.
31. Feng H, Feng J, Zhang Z, Xu Q, Hu M, Wu Y, *et al.* Role of IL-9 and IL-10 in the pathogenesis of chronic spontaneous urticaria through the JAK/STAT signalling pathway. Cell Biochem Funct 2020;38(4):480-9.
32. Mo C, Shetti D, Wei K. Erianin inhibits proliferation and induces apoptosis of HaCaT cells *via* ROS-mediated JNK/c-Jun and AKT/mTOR signaling pathways. Molecules 2019;24(15):2727.
33. Yang S, Liu Y, Guo Y, Liu R, Qi F, Li X, *et al.* Circadian gene Clock participates in mitochondrial apoptosis pathways by regulating mitochondrial membrane potential, mitochondria out membrane permeablization and apoptosis factors in AML12 hepatocytes. Mol Cell Biochem 2020;467:65-75.
34. Mullenders J, Fabius AW, Madiredjo M, Bernards R, Beijersbergen RL. A large scale shRNA barcode screen identifies the circadian clock component ARNTL as putative regulator of the p53 tumor suppressor pathway. PloS One 2009;4(3):e4798.
35. He Q, Wu B, Price JL, Zhao Z. Circadian rhythm neuropeptides in *Drosophila*: Signals for normal circadian function and circadian neurodegenerative disease. Int J Mol Sci 2017;18(4):886.
36. Qin T, Lu XT, Li YG, Liu Y, Yan W, Li N, *et al.* Effect of period 2 on the proliferation, apoptosis and migration of osteosarcoma cells, and the corresponding mechanisms. Oncol Lett 2018;16(2):2668-74.
37. Cohen-Saidon C, Nechushtan H, Kahlon S, Livni N, Nissim A, Razin E. A novel strategy using single-chain antibody to show the importance of Bcl-2 in mast cell survival. Blood 2003;102(7):2506-12.
38. Nakamura Y, Harama D, Shimokawa N, Hara M, Suzuki R, Tahara Y, *et al.* Circadian clock gene Period2 regulates a time-of-day-dependent variation in cutaneous anaphylactic reaction. J Allergy Clin Immunol 2011;127(4):1038-45.
39. Annamneedi VP, Park JW, Lee GS, Kang TJ. Cell autonomous circadian systems and their relation to inflammation. Biomol Ther 2021;29(1):31.
40. Choi JY, Joh HM, Park JM, Kim MJ, Chung TH, Kang TH. Non-thermal plasma-induced apoptosis is modulated by ATR- and PARP1-mediated DNA damage responses and circadian clock. Oncotarget 2016;7(22):32980.
41. Snelling SJ, Forster A, Mukherjee S, Price AJ, Poulsen RC. The chondrocyte-intrinsic circadian clock is disrupted in human osteoarthritis. Chronobiol Int 2016;33(5):574-9.
42. Rong J, Zhu M, Munro J, Cornish J, McCarthy GM, Dalbeth N, *et al.* Altered expression of the core circadian clock component PERIOD2 contributes to osteoarthritis-like changes in chondrocyte activity. Chronobiol Int 2019;36(3):319-31.
43. Baxter M, Ray DW. Circadian rhythms in innate immunity and stress responses. Immunology 2020;161(4):261-7.
44. Miki T, Chen-Goodspeed M, Zhao Z, Lee CC. Circadian behavior of mice deficient in PER1/PML or PER2/PML. J Circadian Rhythms 2013;11(1):1-7.
45. Hartmann MC, McCulley WD, Johnson ST, Salisbury CS, Vaidya N, Smith CG, *et al.* Photic regulation of circadian rhythms and voluntary ethanol intake: Role of melanopsin-expressing intrinsically photosensitive retinal ganglion cells. J Biol Rhythms 2021;36(2):146-59.
46. Ohta K, Yamashita N. Apoptosis of eosinophils and lymphocytes in allergic inflammation. J Allergy Clin Immunol 1999;104(1):14-21.
47. Basti A, Fior R, Yalin M, Povoa V, Astaburuaga R, Li Y. The core-clock gene NR1D1 impacts cell motility *in vitro* and invasiveness in a zebrafish xenograft colon cancer model. Cancers (Basel) 2020;12 (4):853.
48. Hamada T, Niki T, Ishida N. Role of p53 in the entrainment of mammalian circadian behavior rhythms. Genes Cells 2014;19(5):441-8.
49. Jiang W, Zhao S, Jiang X, Zhang E, Hu G, Hu B, *et al.* The circadian clock gene Bmal1 acts as a potential anti-oncogene in pancreatic cancer by activating the p53 tumor suppressor pathway. Cancer Lett 2016;371(2):314-25.
50. Rabinovich-Nikitin I, Lieberman B, Martino TA, Kirshenbaum LA. Circadian-regulated cell death in cardiovascular diseases. Circulation 2019;139(7):965-80.
51. Bonten TN, Saris A, van Oostrom MJ, Snoep JD, Rosendaal FR, Zwaginga JJ, *et al.* Effect of aspirin intake at bedtime *vs.* on awakening on circadian rhythm of platelet reactivity. Thromb Haemost 2014;112(12):1209-18.

This article was originally published in a special issue, "Drug Discovery and Repositioning Studies in Biopharmaceutical Sciences" Indian J Pharm Sci 2024:86(4) Spl Issue "288-300"